Reflection Design Methods for Reconfigurable Intelligent Surfaces-Aided Dynamic TDD Systems

Gerald C. Nwalozie, Khaled Ardah, and Martin Haardt
Communication Research Laboratory
Ilmenau University of Technology - Ilmenau, Germany
Email: {gerald-chetachi.nwalozie, khaled.ardah, martin.haardt}@tu-ilmenau.de

2022 IEEE 12th Sensor Array and Multichannel Signal Processing Workshop (SAM) | 978-1-6654-0633-8/22/$31.00 ©2022 IEEE | DOI: 10.1109/SAM53842.2022.9827850

***Abstract*—Dynamic time-division-duplexing (DTDD) and reconfigurable intelligent surfaces (RISs) have been proposed recently as solutions to meet the small cells traffic fluctuations and to tune the wireless propagation channels in real-time, respectively. However, to the best of the authors' knowledge, there has been no work so far considering the integration of both techniques. Therefore, we consider in this paper an RIS-aided DTDD wireless system and propose two non-iterative methods to design the RIS reflection vector with the objective of maximizing the system spectral efficiency, while reducing the cross-link interference. Numerical results are presented showing the efficiency of the proposed methods as compared to some baseline schemes. It is shown that the integration of RIS in DTDD systems has great potential in improving communication efficiency while reducing the impact of cross-link interference.**

***Index Terms*—Dynamic TDD, MIMO communications, small cells, reconfigurable intelligent surface.**

I. Introduction

Ultra-dense small cells network deployment is one of the key techniques to meet the exponential growth of traffic demands for 5G and future wireless networks. Small cells using low-power nodes are meant to be deployed in hot spots, where the number of users varies strongly with time and between adjacent cells [1]. As a result, small cells are expected to have burst-like traffic, which makes the static time division duplex (TDD) frame configuration strategy, where a common TDD pattern is selected for the whole network, not able to meet the users' requirements and the traffic fluctuations. This inadvertently leads to a high drop rate for the small cells. Dynamic TDD has been proposed as a solution to satisfy the asymmetric and dynamic traffic demand of small cells [2]. In DTDD, each cell is allowed to dynamically reconfigure its TDD pattern based on its instantaneous traffic demand and/or interference status. In [3], the DTDD system performance was evaluated with different performance metrics, and it was found that the DTDD system provides a significant improvement in throughput as compared to the static TDD.

The main challenge brought by DTDD is the cross-link interference issue, because adjacent cells may use at a given time different TDD frame configurations according to traffic needs, thereby giving rise to opposite transmission directions among neighboring cells. There are two kinds of cross-link interference: base station-to-base station (BS-to-BS) and user equipment-to-user equipment (UE-to-UE) interference, which may degrade the system performance significantly. Among the two, the BS-to-BS interference is extremely detrimental due to the large transmit power and line-of-sight (LOS) propagation characteristics. Therefore, there is a need to develop an efficient cross-link interference management scheme.

Recently, reconfigurable intelligent surfaces (RISs) have gained significant attention as a cost-effective solution to improve the current and future wireless networks [4]–[8]. In a passive RIS-aided communication system, where the RIS has no radio-frequency chains, the phase shifts of the RIS elements can be adjusted to meet a certain cost function, e.g., the reflected signals add constructively at the intended users and/or destructively at the unintended users [6]. Due to these potentials, RIS-aided communication systems have received significant attention in the last few years, where various RIS-aided communication systems have been studied, such as millimeter-wave (mmWave) communications, cognitive radio, and unmanned aerial vehicle (UAV) communications [9]–[12].

In this paper, we consider an RIS-aided DTDD system controlled by a central processing unit (CPU) with the aim of investigating the potential benefits of employing the RIS to improve communication efficiency, while reducing the impact of cross-link BS-to-BS interference. To the best of the authors' knowledge, this is the first work that considers the integration of an RIS in a DTDD system. Our main contribution is in the design of the passive RIS reflection vector, where two low-complexity and non-iterative methods are proposed to design the RIS reflection vector with the objective of maximizing the system spectral efficiency (SE), while completely eliminating the cross-link BS-to-BS interference. On the other hand, we adopt the classical zero-forcing (ZF) and minimum mean squared error (MMSE) schemes for the design of active transmit and receive beamforming vectors at the BSs, respectively. Moreover, we assume that the small cells directions are optimized a prior, e.g., using the proposed cell reconfiguration method in [13], and are known at the CPU. Detailed simulation results are provided showing the efficiency of the proposed RIS reflection design methods as compared to some baseline methods. Specifically, it is shown that the integration of RISs in DTDD systems has a great potential in improving communication spectral efficiency by providing alternative and extra communication links, while at the same time reducing the impact of the cross-link BS-to-BS interference.

II. System Model

In this paper[1], we consider an RIS-aided mmWave DTDD system consisting of Q small cells, where each cell has a BS with a uniform linear array (ULA) of N antennas serving a single UE[2] that is equipped with a single-antenna. As shown in Fig. 1, we assume that the communication is aided by an RIS with M passive reflection elements, where the BSs and the RIS are controlled by a central processing unit (CPU) via backhaul connections. Let $\mathcal{Q} \triangleq \{1, \cdots, Q\}$ denote the set of BSs (cells). At the considered time instant, we assume that there are $|\mathcal{Q}^{\text{ul}}|$ cells operating in the uplink (UL) direction and $|\mathcal{Q}^{\text{dl}}|$ cells operating in the downlink (DL) direction, such that $|\mathcal{Q}^{\text{ul}}| + |\mathcal{Q}^{\text{dl}}| = Q$ and $\mathcal{Q}^{\text{ul}} \bigcap \mathcal{Q}^{\text{dl}} = \emptyset$.

Let $\mathbf{H}_q \in \mathbb{C}^{M\times N}$ be the channel matrix from the qth BS to the RIS, $\mathbf{h}_q \in \mathbb{C}^M$ be the channel vector from the qth UE to the RIS, $\mathbf{G}_{r,q} \in \mathbb{C}^{N\times N}$ be the channel matrix from the qth BS to the rth BS, $\mathbf{g}_{r,q} \in \mathbb{C}^N$ be the channel vector from the qth BS to the rth UE, and $g_{r,q} \in \mathbb{C}$ be the channel scalar from qth UE to the rth UE. Then, the received signal by the UE in the qth DL cell, i.e., $q \in \mathcal{Q}^{\text{dl}}$, can be expressed as

$$y_q^{(\text{dl})} = \sum_{\forall k\in\mathcal{Q}^{\text{dl}}} (\mathbf{h}_{q,k}^{\text{BS-UE}})^{\mathsf{T}} \mathbf{f}_k x_k + \sum_{\forall r\in\mathcal{Q}^{\text{ul}}} h_{q,r}^{\text{UE-UE}} \sqrt{p_r^{\text{ul}}} x_r + z_q, \quad (1)$$

where $\mathbf{h}_{q,k}^{\text{BS-UE}} = (\mathbf{h}_q^{\mathsf{T}} \boldsymbol{\Theta} \mathbf{H}_k + \mathbf{g}_{q,k}^{\mathsf{T}})^{\mathsf{T}}$, $h_{q,r}^{\text{UE-UE}} = \mathbf{h}_q^{\mathsf{T}} \boldsymbol{\Theta} \mathbf{h}_r + g_{q,r}$, $\boldsymbol{\Theta} = \text{diag}(\boldsymbol{\theta})$ is the RIS reflection diagonal matrix, $\boldsymbol{\theta} = [e^{j\phi_1}, \cdots, e^{j\phi_M}]^{\mathsf{T}} \in \mathbb{C}^M$ with $\phi_m \in [0, 2\pi]$, $\mathbf{f}_k \in \mathbb{C}^N$ is the transmit precoding vector with $\|\mathbf{f}_k\|_2^2 = p_k^{\text{dl}}$, x_k is the unit-norm transmit symbol, z_q is additive white Gaussian noise with variance σ_q^2, and p_r^{X} is the transmit power at the $\text{X} \in \{\text{dl}, \text{ul}\}$ direction. Therefore, the signal-to-interference-plus-noise ratio (SINR) of the qth UE, $q \in \mathcal{Q}^{\text{dl}}$, is given as

$$\Gamma_q^{(\text{dl})} = \frac{|(\mathbf{h}_{q,q}^{\text{BS-UE}})^{\mathsf{T}} \mathbf{f}_q|^2}{\sum\limits_{\substack{\forall k\in\mathcal{Q}^{\text{dl}}\\ k\neq q}} |(\mathbf{h}_{q,k}^{\text{BS-UE}})^{\mathsf{T}} \mathbf{f}_k|^2 + \sum\limits_{\forall r\in\mathcal{Q}^{\text{ul}}} |h_{q,r}^{\text{BS-UE}}|^2 p_r^{\text{ul}} + \sigma_q^2}. \quad (2)$$

On the other hand, the received signal at the rth UL BS, i.e., $r \in \mathcal{Q}^{\text{ul}}$, after the receive combining, can be expressed as

$$y_r^{(\text{ul})} = \sum_{\forall j\in\mathcal{Q}^{\text{ul}}} \mathbf{w}_r^{\mathsf{H}} \mathbf{h}_{r,j}^{\text{BS-UE}} \sqrt{p_j^{\text{ul}}} x_j + \sum_{\forall q\in\mathcal{Q}^{\text{dl}}} \mathbf{w}_r^{\mathsf{H}} \mathbf{H}_{r,q}^{\text{BS-BS}} \mathbf{f}_q x_q + \tilde{z}_r, \quad (3)$$

where $\mathbf{H}_{r,q}^{\text{BS-BS}} = \mathbf{H}_r^{\mathsf{T}} \boldsymbol{\Theta} \mathbf{H}_q + \mathbf{G}_{r,q}$, $\mathbf{w}_r \in \mathbb{C}^N$ is the receive decoding vector with $\|\mathbf{w}_r\|_2^2 = 1$, $\tilde{z}_r = \mathbf{w}_r^{\mathsf{H}} \mathbf{z}_r$ with $\mathbf{z}_r \in \mathbb{C}^N$ being the additive white Gaussian noise with variance σ_r^2. Therefore, the SINR for the rth UE, $r \in \mathcal{Q}^{\text{ul}}$, is given as

$$\Gamma_r^{(\text{ul})} = \frac{|\mathbf{w}_r^{\mathsf{H}} \mathbf{h}_{r,r}^{\text{BS-UE}}|^2 p_r^{\text{ul}}}{\sum\limits_{\substack{\forall j\in\mathcal{Q}^{\text{ul}}\\ j\neq r}} |\mathbf{w}_r^{\mathsf{H}} \mathbf{h}_{r,j}^{\text{BS-UE}}|^2 p_j^{\text{ul}} + \sum\limits_{\forall q\in\mathcal{Q}^{\text{dl}}} |\mathbf{w}_r^{\mathsf{H}} \mathbf{H}_{r,q}^{\text{BS-BS}} \mathbf{f}_q|^2 + \sigma_r^2}. \quad (4)$$

From the above, the system SE is given as

$$\text{SE} = \sum_{\forall q\in\mathcal{Q}^{\text{dl}}} \log_2\left(1 + \Gamma_q^{(\text{dl})}\right) + \sum_{\forall r\in\mathcal{Q}^{\text{ul}}} \log_2\left(1 + \Gamma_r^{(\text{ul})}\right). \quad (5)$$

In this paper, we assume that the above defined channel matrices $\{\mathbf{H}_q, \mathbf{h}_q, \mathbf{G}_{r,q}, \mathbf{g}_{r,q}, g_{r,q}\}$ are modeled according to the well-known mmWave Saleh-Valenzuela geometric channel model [14], where every channel is modeled as a summation of $L \ll \max\{M, N\}$ paths, each has a distinctive direction-of-departure (DoD) and/or direction-of-arrival (DoA) and a complex path gain. Under this assumption, we have that $\text{rank}\{\mathbf{H}_q\} \leq L, \forall q$ and $\text{rank}\{\mathbf{G}_{r,q}\} \leq L, \forall r, q$. Due to space limitations, we omit the channel modeling here and refer to [8]–[10] for more details. Moreover, we assume that the channels are static and known at the BSs through the CPU.

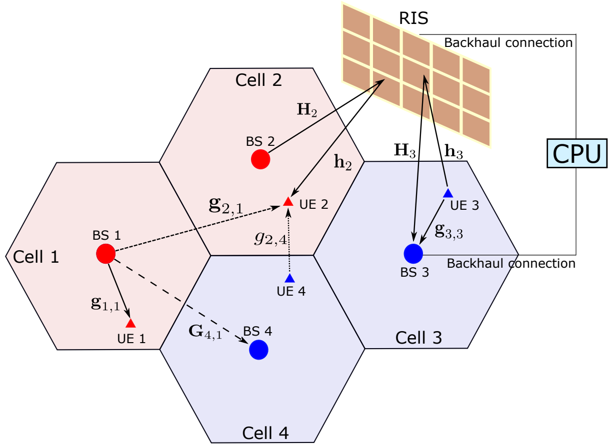

Fig. 1: An RIS-aided DTDD system comprising $Q = 4$ cells.

III. Problem Formulation

Our main goal is to design the passive reflection vector of the RIS and the active transmit and receive beamforming vectors of the BSs to maximize the system SE, which can be formulated as

$$\begin{aligned} \max_{\mathbf{f}_q, \forall q\in\mathcal{Q}^{\text{dl}}, \mathbf{w}_r, \forall r\in\mathcal{Q}^{\text{ul}}, \boldsymbol{\theta}} \quad & \text{SE} \\ \text{s.t} \quad & (\text{C1}): \|\mathbf{f}_q\|_2^2 = p_q^{\text{dl}}, \ \forall q \in \mathcal{Q}^{\text{dl}} \\ & (\text{C2}): |[\boldsymbol{\theta}]_{[m]}|^2 = 1, \ m = 1, \cdots, M, \end{aligned} \quad (6)$$

where (C1) is the DL transmit power constraint and (C2) are the constant modulus constraints (CMCs) for the RIS reflection coefficients. Problem (6) is non-convex due to its joint optimization and the CMCs in (C2). To obtain a solution, we propose in the following non-iterative solutions by decoupling the optimization between the problem variables. Specifically, given the channel matrices, we propose two solution methods for the design of the RIS passive reflection vector $\boldsymbol{\theta} \in \mathbb{C}^M$. After that, for a given $\boldsymbol{\theta}$, we design the BSs' transmit and receive active beamformers $\mathbf{f}_q, \forall q \in \mathcal{Q}^{\text{dl}}$, and $\mathbf{w}_r, \forall r \in \mathcal{Q}^{\text{ul}}$, using the classical ZF and MMSE methods, respectively.

[1] *Notation:* Vectors and matrices are written as lowercase and uppercase boldface letters, respectively. The notation $\diamond$ is used to denote the Khatri-Rao product. The transpose and the conjugate transpose (Hermitian) of $\mathbf{X}$ are represented by $\mathbf{X}^{\mathsf{T}}$ and $\mathbf{X}^{\mathsf{H}}$, respectively. The $\text{diag}(\mathbf{x})$ forms a matrix by placing $\mathbf{x}$ on its main diagonal, and $\text{vec}(\mathbf{X})$ vectorizes $\mathbf{X}$ by stacking its columns on top of each other. The following property is used: Property-1: $\text{vec}(\mathbf{A}\text{diag}(\mathbf{b})\mathbf{C}) = (\mathbf{C}^{\mathsf{T}} \diamond \mathbf{A})\mathbf{b}$.

[2] The extension of our proposed solution to multi-user scenarios is straightforward.

IV. Proposed RIS Reflection Design Methods

From Property 1, we first note that the vectorized form of the above defined effective channels can be expressed as

$$\mathbf{h}_{q,k}^{\text{BS-UE}} = \mathbf{H}_{q,k}^{\text{BS-UE}}\boldsymbol{\theta} + \mathbf{g}_{q,k} \tag{7}$$

$$\text{vec}\{\mathbf{H}_{r,q}^{\text{BS-BS}}\} = \mathbf{H}_{r,q}^{\text{BS-BS}}\boldsymbol{\theta} + \text{vec}\{\mathbf{G}_{r,q}\} \tag{8}$$

$$h_{q,r}^{\text{UE-UE}} = \mathbf{h}_{q,r}^{\text{UE-UE}}\boldsymbol{\theta} + g_{q,r}, \tag{9}$$

where we define $\mathbf{H}_{q,k}^{\text{BS-UE}} = (\mathbf{H}_k^\mathsf{T} \diamond \mathbf{h}_q^\mathsf{T}) \in \mathbb{C}^{N\times M}$, $\mathbf{H}_{r,q}^{\text{BS-BS}} = (\mathbf{H}_q^\mathsf{T} \diamond \mathbf{H}_r^\mathsf{T}) \in \mathbb{C}^{N^2\times M}$, and $\mathbf{h}_{q,r}^{\text{UE-UE}} = (\mathbf{h}_r^\mathsf{T} \diamond \mathbf{h}_q^\mathsf{T}) \in \mathbb{C}^{1\times M}$. Note that $\text{rank}\{\mathbf{H}_{q,k}^{\text{BS-UE}}\} \leq L$, $\text{rank}\{\mathbf{H}_{r,q}^{\text{BS-BS}}\} \leq L^2$, and $\text{rank}\{\mathbf{h}_{q,r}^{\text{UE-UE}}\} = 1$. Moreover, from the signal models in (1) and (3), we know that the effective channels $\{\mathbf{h}_{q,k}^{\text{BS-UE}}\}$ carry the desired signals (DS) and the inter-cell interference (ICI) signal, while $\{\mathbf{H}_{q,k}^{\text{BS-BS}}, h_{q,r}^{\text{UE-UE}}\}$ carry the cross-link (CL) interference signals. Therefore, we define the following matrices

$$\mathbf{D}_{\text{DS}}^{\text{BS-UE}} = \text{stack}\{\mathbf{H}_{q,q}^{\text{BS-UE}}\}_{\forall q\in\mathcal{Q}} \tag{10}$$

$$\mathbf{C}_{\text{DL-ICI}}^{\text{BS-UE}} = \text{stack}\{\mathbf{H}_{q,k}^{\text{BS-UE}}\}_{\forall k,q\in\mathcal{Q}^{\text{dl}},k\neq q} \tag{11}$$

$$\mathbf{C}_{\text{UL-ICI}}^{\text{BS-UE}} = \text{stack}\{\mathbf{H}_{q,k}^{\text{BS-UE}}\}_{\forall k,q\in\mathcal{Q}^{\text{ul}},k\neq q} \tag{12}$$

$$\mathbf{C}_{\text{DL-CL}}^{\text{BS-BS}} = \text{stack}\{\mathbf{H}_{r,q}^{\text{BS-BS}}\}_{\forall r\mathcal{Q}^{\text{ul}},\forall q\in\mathcal{Q}^{\text{dl}}} \tag{13}$$

$$\mathbf{C}_{\text{UL-CL}}^{\text{UE-UE}} = \text{stack}\{\mathbf{h}_{q,r}^{\text{UE-UE}}\}_{\forall r\mathcal{Q}^{\text{ul}},\forall q\in\mathcal{Q}^{\text{dl}}}, \tag{14}$$

where we define $\mathbf{A} = \text{stack}\{\mathbf{A}_i\}_{\forall i\in\mathcal{I}} = [\mathbf{A}_1^\mathsf{T}, \cdots, \mathbf{A}_{|\mathcal{I}|}^\mathsf{T}]^\mathsf{T}$, i.e., a function that stacks the input matrices over each other. From the above, we propose to design the RIS reflection vector $\boldsymbol{\theta} \in \mathbb{C}^M$ as a solution to

$$\begin{aligned} \max_{\boldsymbol{\theta}} \quad & \|\mathbf{D}_{\text{DS}}^{\text{BS-UE}}\boldsymbol{\theta}\|_2^2 \\ \text{s.t} \quad & (\text{C2}): |[\boldsymbol{\theta}]_{[m]}|^2 = 1,\ m = 1,\cdots,M \\ & (\text{C3}): \mathbf{C}_{\text{ICI-CL}}\boldsymbol{\theta} = \mathbf{0} \end{aligned} \tag{15}$$

in which $\mathbf{C}_{\text{ICI-CL}} = \text{stack}\{\mathbf{C}_{\text{DL-ICI}}^{\text{BS-UE}}, \mathbf{C}_{\text{UL-ICI}}^{\text{BS-UE}}, \mathbf{C}_{\text{DL-CL}}^{\text{BS-BS}}, \mathbf{C}_{\text{UL-CL}}^{\text{UE-UE}}\}$. The problem in (15) is non-convex due to CMCs in (C2). In the following, we propose two non-iterative solutions to obtain a feasible and efficient RIS reflection vector.

Remark 1: Given the above mmWave channel modeling, then the following inequality holds true:

$$\text{rank}\{\mathbf{C}_{\text{ICI-CL}}\} \leq L_{\text{DL-ICI}}^{\text{BS-UE}} + L_{\text{UL-ICI}}^{\text{BS-UE}} + L_{\text{DL-CL}}^{\text{BS-BS}} + L_{\text{UL-CL}}^{\text{UE-UE}}, \tag{16}$$

where $L_{\text{DL-ICI}}^{\text{BS-UE}} \leq (|\mathcal{Q}^{\text{dl}}|^2 - |\mathcal{Q}^{\text{dl}}|)L$, from (11), $L_{\text{UL-ICI}}^{\text{BS-UE}} \leq (|\mathcal{Q}^{\text{ul}}|^2 - |\mathcal{Q}^{\text{ul}}|)L$, from (12), $L_{\text{DL-CL}}^{\text{BS-BS}} \leq |\mathcal{Q}^{\text{dl}}||\mathcal{Q}^{\text{ul}}|L^2$, from (13), and $L_{\text{UL-CL}}^{\text{UE-UE}} \leq |\mathcal{Q}^{\text{dl}}||\mathcal{Q}^{\text{ul}}|$, from (14).

Method 1: In this method, we relax (15) and write it as

$$\begin{aligned} \max_{\boldsymbol{\theta}} \quad & \|\mathbf{D}_{\text{DS}}^{\text{BS-UE}}\boldsymbol{\theta}\|_2^2 \\ \text{s.t} \quad & (\text{C3}): \mathbf{C}_{\text{ICI-CL}}\boldsymbol{\theta} = \mathbf{0} \\ & (\text{C4}): \|\boldsymbol{\theta}\|_2^2 = 1. \end{aligned} \tag{17}$$

A direct solution to (17) is given as

$$\boldsymbol{\theta}^{\text{FD-1}} = \mathbf{V}_{\text{ICI-CL}}^{\text{NS}}\mathbf{v}_{\max}^{\text{DS}} \in \mathbb{C}^M, \tag{18}$$

where $\mathbf{V}_{\text{ICI-CL}}^{\text{NS}}$ holds the basis for the null-space (NS) of $\mathbf{C}_{\text{ICI-CL}}$, which can be obtained from the singular value decomposition (SVD) of $\mathbf{C}_{\text{ICI-CL}}$ [15] and $\mathbf{v}_{\max}^{\text{DS}}$ is the right singular vector corresponding to the maximum singular value of $\mathbf{D}_{\text{DS}}^{\text{BS-UE}}\mathbf{V}_{\text{ICI-CL}}^{\text{NS}}$. Therefore, a solution to (15) is given as

$$\boldsymbol{\theta}^{\text{CMC-1}} \longleftarrow \text{P}\left(\boldsymbol{\theta}^{\text{FD-1}}\right), \tag{19}$$

where $\text{P}(z_i) = \frac{z_i}{|z_i|}$ is the element-wise projection function.

Method 2: In this method, we propose to solve (17) by first assuming that $\boldsymbol{\theta}$ is decomposed into Q sub-vectors as

$$\boldsymbol{\theta} = \boldsymbol{\theta}_1 + \boldsymbol{\theta}_2 + \cdots + \boldsymbol{\theta}_Q, \tag{20}$$

where $\|\boldsymbol{\theta}_q\|_2^2 = 1, \forall q$. Given the above decomposition, we propose to design the qth sub-vector $\boldsymbol{\theta}_q$ as

$$\begin{aligned} \max_{\boldsymbol{\theta}_q} \quad & \|\mathbf{H}_{q,q}^{\text{BS-UE}}\boldsymbol{\theta}_q\|_2^2 \\ \text{s.t} \quad & (\text{C4}): \|\boldsymbol{\theta}_q\|_2^2 = 1 \\ & (\text{C5}): \boldsymbol{\Pi}_q^{\text{INT}}\boldsymbol{\theta}_q = \mathbf{0}, \end{aligned} \tag{21}$$

where $\boldsymbol{\Pi}_q^{\text{INT}} = \text{stack}\{\mathbf{D}_{\text{DS-INT}}^{\text{BS-UE}}, \mathbf{C}_{\text{ICI-CL}}\}$ and

$$\mathbf{D}_{\text{DS-INT}}^{\text{BS-UE}} = \text{stack}\{\mathbf{H}_{r,r}^{\text{BS-UE}}\}_{\forall r\in\mathcal{Q},r\neq q}, \tag{22}$$

i.e., a matrix containing all blocks of $\mathbf{D}_{\text{DS}}^{\text{BS-UE}}$ in (10) except for the qth sub-block. Note that $\text{rank}\{\boldsymbol{\Pi}_q^{\text{INT}}\} \leq \text{rank}\{\mathbf{C}_{\text{ICI-CL}}\} + L_{\text{DS-INT}}^{\text{BS-UE}}$, where $L_{\text{DS-INT}}^{\text{BS-UE}} \leq (Q-1)L$. A solution to the qth sub-problem in (21) is given as

$$\boldsymbol{\theta}_q^{\text{FD-2}} = \mathbf{V}_{\text{INT},q}^{\text{NS}}\mathbf{v}_{\max,q}^{\text{BS-UE}} \in \mathbb{C}^M, \tag{23}$$

where $\mathbf{V}_{\text{INT},q}^{\text{NS}}$ holds the basis for the null-space (NS) of $\boldsymbol{\Pi}_q^{\text{INT}}$, and $\mathbf{v}_{\max,q}^{\text{BS-UE}}$ is the right singular vector corresponding to the maximum singular value of $\mathbf{H}_{q,q}^{\text{BS-UE}}\mathbf{V}_{\text{INT},q}^{\text{NS}}$. Let $\boldsymbol{\Theta}^{\text{FD-2}} = [\boldsymbol{\theta}_1^{\text{FD-2}}, \cdots, \boldsymbol{\theta}_Q^{\text{FD-2}}] \in \mathbb{C}^{M\times Q}$. Then, it can be easily shown that

$$\mathbf{D}_{\text{DS}}^{\text{BS-UE}}\boldsymbol{\Theta}^{\text{FD-2}} = \begin{bmatrix} \mathbf{e}_1 & \cdots & \mathbf{0} \\ \vdots & \ddots & \vdots \\ \mathbf{0} & \cdots & \mathbf{e}_Q \end{bmatrix} \in \mathbb{C}^{QN\times Q}, \tag{24}$$

where $\boldsymbol{e}_q \in \mathbb{R}^N$. Let $\boldsymbol{\theta}^{\text{FD-2}} = \frac{\boldsymbol{\theta}_1^{\text{FD-2}} + \cdots + \boldsymbol{\theta}_Q^{\text{FD-2}}}{\|\boldsymbol{\theta}_1^{\text{FD-2}} + \cdots + \boldsymbol{\theta}_Q^{\text{FD-2}}\|}$, then we have,

$$\mathbf{D}_{\text{DS}}^{\text{BS-UE}}\boldsymbol{\theta}^{\text{FD-2}} = \text{stack}\{\bar{\mathbf{e}}_1, \ldots, \bar{\mathbf{e}}_Q\}, \tag{25}$$

where $\bar{\mathbf{e}}_q = \frac{\mathbf{e}_q}{\|\boldsymbol{\theta}_1^{\text{FD-2}} + \cdots + \boldsymbol{\theta}_Q^{\text{FD-2}}\|}$. Finally, to satisfy the constant modulus constraints of (C2) in (15), we apply the projection function as

$$\boldsymbol{\theta}^{\text{CMC-2}} \longleftarrow \text{P}\left(\boldsymbol{\theta}^{\text{FD-2}}\right). \tag{26}$$

V. Transmit and Receive Beamforming Design

For a given $\boldsymbol{\theta}$, e.g., $\boldsymbol{\theta} \in \{\boldsymbol{\theta}^{\text{CMC-1}}, \boldsymbol{\theta}^{\text{CMC-2}}\}$, we design the transmit and the receive beamforming vectors $\mathbf{f}_q, \forall q \in \mathcal{Q}^{\text{dl}}$, and $\mathbf{w}_r, \forall r \in \mathcal{Q}^{\text{ul}}$. Specifically, the qth transmit vector $\mathbf{f}_q, q \in \mathcal{Q}^{\text{dl}}$, is designed to satisfy the following interference condition

$$\boldsymbol{\Upsilon}_q\mathbf{f}_q = \mathbf{0}, \forall q \in \mathcal{Q}^{\text{dl}}, \tag{27}$$

where $\boldsymbol{\Upsilon}_q = \text{stack}\{\boldsymbol{\Upsilon}_q^{\text{ICI}}, \boldsymbol{\Upsilon}_q^{\text{BS-BS}}\}$ is a matrix collecting the *direct* interference channels relative to the qth UE, where

$$\boldsymbol{\Upsilon}_q^{\text{ICI}} = \text{stack}\{\mathbf{g}_{r,q}^\mathsf{T}\}_{\forall r\in\mathcal{Q}^{\text{dl}},r\neq q} \tag{28}$$

$$\boldsymbol{\Upsilon}_q^{\text{BS-BS}} = \text{stack}\{\mathbf{G}_{r,q}\}_{\forall r\in\mathcal{Q}^{\text{ul}}}. \tag{29}$$

which satisfies $\text{rank}\{\boldsymbol{\Upsilon}_q\} \leq (|\mathcal{Q}^{\text{dl}}| - 1) + |\mathcal{Q}^{\text{ul}}|L$. Given $\boldsymbol{\Upsilon}_q$, the qth transmit vector $\mathbf{f}_q, q \in \mathcal{Q}^{\text{dl}}$, is given as

$$\mathbf{f}_q = \frac{\bar{\mathbf{f}}_q}{\|\bar{\mathbf{f}}_q\|_2}\sqrt{p_q^{\text{dl}}}, \tag{30}$$

where $\bar{\mathbf{f}}_q = \mathbf{V}_q^{\text{NS}}\mathbf{v}_{\max,q}$, in which $\mathbf{V}_q^{\text{NS}}$ holds the basis for the null-space of $\boldsymbol{\Upsilon}_q$, while $\mathbf{v}_{\max,q}$ is the right singular vector corresponding to the maximum singular value of $(\mathbf{h}_{q,q}^{\text{BS-UE}})^\mathsf{T}\mathbf{V}_q^{\text{NS}}$.

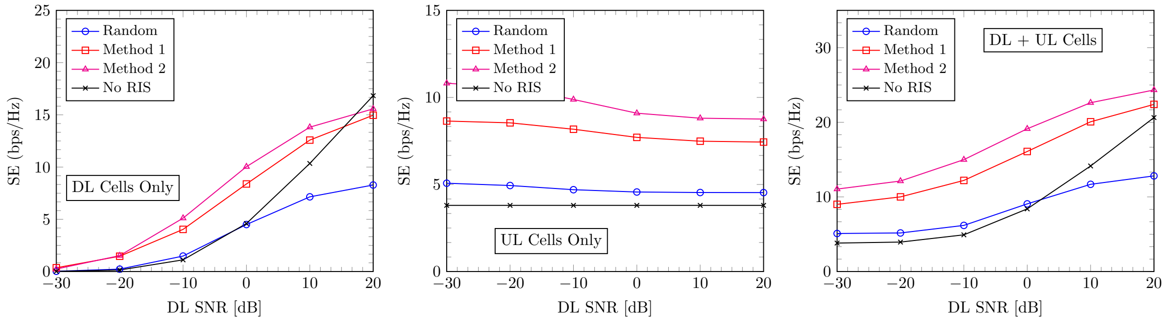

Fig. 2: SE versus DL SNR, assuming $M = 256$ and $N = 16$.

On the other hand, we design the rth decoding vector $\mathbf{w}_r, r \in \mathcal{Q}^{\text{ul}}$, using the MMSE scheme [16], which is given as

$$\mathbf{w}_{\text{MMSE},r} = \frac{\mathbf{B}_r^{-1}\mathbf{h}_{r,r}^{\text{BS-UE}}}{\|\mathbf{B}_r^{-1}\mathbf{h}_{r,r}^{\text{BS-UE}}\|_2}, \forall r \in \mathcal{Q}^{\text{ul}}, \tag{31}$$

where

$$\mathbf{B}_r = \sum_{\forall j \in \mathcal{Q}^{\text{ul}}} p_r^{\text{ul}} \mathbf{h}_{r,j}^{\text{BS-UE}} (\mathbf{h}_{r,j}^{\text{BS-UE}})^{\text{H}} + \sum_{\forall q \in \mathcal{Q}^{\text{dl}}} \mathbf{H}_{r,q}^{\text{BS-BS}} \mathbf{f}_{\text{ZF},q} (\mathbf{H}_{r,q}^{\text{BS-BS}} \mathbf{f}_{\text{ZF},q})^{\text{H}} + \sigma_r^2 \boldsymbol{I}_N.$$

Complexity analysis: Since the complexity of computing the SVD of a $m \times n$ matrix, with $m \geq n$, is in the order of $\mathcal{O}\{n^2\}$, then the complexity of calculating $\boldsymbol{\theta}^{\text{CMC-1}}$ is in the order of $\mathcal{O}\{M^2\}$, $\boldsymbol{\theta}^{\text{CMC-2}}$ is in the order of $\mathcal{O}\{QM^2\}$, and the transmit precoding vectors $\mathbf{f}_q, \forall q \in \mathcal{Q}^{\text{dl}}$, is in the order of $\mathcal{O}\{|\mathcal{Q}^{\text{dl}}|N^2\}$. Moreover, the complexity of calculating the decoding vectors $\mathbf{w}_r, \forall r \in \mathcal{Q}^{\text{ul}}$, is in the order of $\mathcal{O}\{|\mathcal{Q}^{\text{ul}}|N^3\}$, since the complexity of computing the inverse of a $n \times n$ matrix is in the order of $\mathcal{O}\{n^3\}$.

VI. Numerical Results

In this section, we show simulation results to evaluate the performance of our proposed methods as compared to baseline schemes. We consider a system with $Q = 4$ cells, as shown in Fig. 1, where $|\mathcal{Q}^{\text{dl}}| = 2$ and $|\mathcal{Q}^{\text{ul}}| = 2$. We set $p_r^{\text{ul}} =$ 23dBm and assume that the number of channels paths $L = 4$, where the corresponding DoDs and/or DoAs are uniformly distributed with $[0, 2\pi]$. We normalize every channel path gains so that $\mathbb{E}\{\|\mathbf{H}_q\|_{\text{F}}^2\} = NM$, $\mathbb{E}\{\|\mathbf{G}_{r,q}\|_{\text{F}}^2\} = N^2$, $\mathbb{E}\{\|\mathbf{h}_q\|_{\text{F}}^2\} = M$, and $\mathbb{E}\{\|\mathbf{g}_{r,q}\|_{\text{F}}^2\} = N$. We include results for the following two baseline cases: 1) Random, where the entries of the RIS reflection vector are designed randomly as $[\boldsymbol{\theta}]_{[m]} = e^{j\phi_m}, \forall m$, with $\phi_m \in [0, 2\pi]$, and 2) No RIS, the case where no RIS is deployed, i.e., $[\boldsymbol{\theta}]_{[m]} = 0, \forall m$.

In Fig. 2, we show the SE versus the DL SNR, while assuming that the RIS has $M = 256$ passive reflecting elements and each BS has $N = 16$ antennas. We plot the achievable SE of the DL and the UL cells separately and then combined to better understand the difference between the proposed and the baseline methods. From the figure, we can clearly see that Method 2 has better SE performance compared to Method 1 and the other two baseline schemes, while both the proposed methods have significantly better performance compared to the Random RIS scenarios. Moreover, we can see from Fig. 3 that the performance advantage of Method 2 compared to the other methods increases as the number of antennas N and the number of the RIS elements M increases.

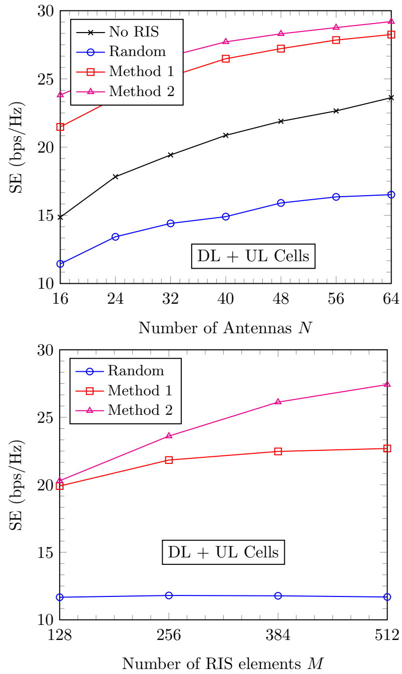

Fig. 3: SE versus number of antennas N for $M = 252$ and SE versus number of RIS elements M for $N = 16$, assuming DL SNR = 10 dB

VII. Conclusions

In this paper, we have considered the active and passive beamforming design problem in an RIS-aided DTDD wireless network to maximize the system spectral efficiency. We have proposed centralized low-complexity and non-iterative solutions for the design of the RIS reflection vector. The provided simulation results have shown that the integration of RISs in DTDD systems has a great potential in improving communication spectral efficiency by providing alternative and extra communication links, while at the same time reducing the impact of the cross-link BS-to-BS interference.

Acknowledgments

This work was supported by Nnamdi Azikiwe University Nigeria, under NEEDS Assessment Fund and the Communication Research Laboratory, Ilmenau University of Technology, Germany .

References

[1] T. Nakamura, S. Nagata, A. Benjebbour, Y. Kishiyama, T. Hai, S. Xiaodong, Y. Ning, and L. Nan, "Trends in small cell enhancements in lte advanced," *IEEE Communications Magazine*, vol. 51, no. 2, pp. 98–105, 2013.

[2] 3GPP, "Evolved Universal Terrestrial Radio Access (E-UTRA): Further enhancements to LTE Time Division Duplex (TDD) for Downlink-Uplink (DL-UL) interference management and traffic adaptation," Tech. Rep. TS 36.828, Jun 2012.

[3] C. Wang, X. Hou, A. Harada, S. Yasukawa, and H. Jiang, "Harq signalling design for dynamic tdd system," in *Proc 2014 IEEE 80th Vehicular Technology Conference (VTC2014-Fall)*, 2014, pp. 1–5.

[4] M. Di Renzo, A. Zappone, M. Debbah, M.-S. Alouini, C. Yuen, J. de Rosny, and S. Tretyakov, "Smart radio environments empowered by reconfigurable intelligent surfaces: How it works, state of research, and the road ahead," *IEEE Journal on Selected Areas in Communications*, vol. 38, no. 11, pp. 2450–2525, 2020.

[5] Q. Wu and R. Zhang, "Towards smart and reconfigurable environment: Intelligent reflecting surface aided wireless network," *IEEE Communications Magazine*, vol. 58, no. 1, pp. 106–112, 2020.

[6] Q. Wu, S. Zhang, B. Zheng, C. You, and R. Zhang, "Intelligent reflecting surface-aided wireless communications: A tutorial," *IEEE Transactions on Communications*, vol. 69, no. 5, pp. 3313–3351, 2021.

[7] S. Gong, X. Lu, D. T. Hoang, D. Niyato, L. Shu, D. I. Kim, and Y.-C. Liang, "Toward smart wireless communications via intelligent reflecting surfaces: A contemporary survey," *IEEE Communications Surveys Tutorials*, vol. 22, no. 4, pp. 2283–2314, 2020.

[8] S. Gherekhloo, K. Ardah, A. L. F. de Almeida, and M. Haardt, "Tensor-based channel estimation and beamforming design for RIS-aided millimeter-wave MIMO systems," in *Proc. of 55th Asilomar Conf. on Signals, Systems, and Computers (Asilomar 2021)*, 2021.

[9] Y. Cao, T. Lv, Z. Lin, and W. Ni, "Delay-constrained joint power control, user detection and passive beamforming in intelligent reflecting surface-assisted uplink mmwave system," *IEEE Transactions on Cognitive Communications and Networking*, vol. 7, no. 2, pp. 482–495, 2021.

[10] K. Ardah, S. Gherekhloo, A. L. F. de Almeida, and M. Haardt, "TRICE: A Channel Estimation Framework for RIS-Aided Millimeter-Wave MIMO Systems," *IEEE Signal Processing Letters*, vol. 28, pp. 513–517.

[11] J. Yuan, Y.-C. Liang, J. Joung, G. Feng, and E. G. Larsson, "Intelligent reflecting surface-assisted cognitive radio system," *IEEE Transactions on Communications*, vol. 69, no. 1, pp. 675–687, 2021.

[12] A. Taha, M. Alrabeiah, and A. Alkhateeb, "Enabling large intelligent surfaces with compressive sensing and deep learning," *IEEE Access*, vol. 9, pp. 44 304–44 321, 2021.

[13] K. Ardah, G. Fodor, Y. C. B. Silva, W. C. Freitas, and F. R. P. Cavalcanti, "A novel cell reconfiguration technique for dynamic tdd wireless networks," *IEEE Wireless Communications Letters*, vol. 7, no. 3, pp. 320–323, 2018.

[14] A. A. M. Saleh and R. Valenzuela, "A statistical model for indoor multipath propagation," *IEEE J. Sel. Areas Commun.*, vol. 5, no. 2, pp. 128–137, Feb. 1987.

[15] Q. Spencer, A. Swindlehurst, and M. Haardt, "Zero-forcing methods for downlink spatial multiplexing in multiuser mimo channels," *IEEE Transactions on Signal Processing*, vol. 52, no. 2, pp. 461–471, 2004.

[16] C.-Y. Hung and W.-H. Chung, "An improved mmse-based mimo detection using low-complexity constellation search," in *2010 IEEE Globecom Workshops*, 2010, pp. 746–750.